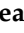



Article

ZnO/Ag₃PO₄ and ZnO–Malachite as Effective Photocatalysts for the Removal of Enteropathogenic Bacteria, Dyestuffs, and Heavy Metals from Municipal and Industrial Wastewater

Julie Joseane Murcia ¹, Jhon Sebastián Hernández Niño ¹, Hugo Rojas ¹, María Helena Brijaldo ^{1,2}, Andrés Noel Martín-Gómez ³, Pablo Sánchez-Cid ³, José Antonio Navío ³, María Carmen Hidalgo ³ and César Jaramillo-Paez ^{4,*}



Citation: Murcia, J.J.; Hernandez Niño, J.S.; Rojas, H.; Brijaldo, M.H.; Martín-Gómez, A.N.; Sánchez-Cid, P.; Navío, J.A.; Hidalgo, M.C.; Jaramillo-Paez, C. ZnO/Ag₃PO₄ and ZnO–Malachite as Effective Photocatalysts for the Removal of Enteropathogenic Bacteria, Dyestuffs, and Heavy Metals from Municipal and Industrial Wastewater. *Water* **2021**, *13*, 2264. <https://doi.org/10.3390/w13162264>

Academic Editors: Changseok Han, Daphne Hermosilla Redondo, Hodon Ryu, Woo Hyoung Lee and Miguel Angel Mueses

Received: 23 July 2021

Accepted: 13 August 2021

Published: 19 August 2021

Publisher's Note: MDPI stays neutral with regard to jurisdictional claims in published maps and institutional affiliations.



Copyright: © 2021 by the authors. Licensee MDPI, Basel, Switzerland. This article is an open access article distributed under the terms and conditions of the Creative Commons Attribution (CC BY) license (<https://creativecommons.org/licenses/by/4.0/>).

- ¹ Grupo de Catálisis, Escuela de Ciencias Químicas, Universidad Pedagógica y Tecnológica de Colombia UPTC, Avenida Central del Norte, Boyacá, Tunja 150003, Colombia; julie.murcia@uptc.edu.co (J.J.M.); sebashernandez94.sh@gmail.com (J.S.H.N.); hugo.rojas@uptc.edu.co (H.R.); maria.brijaldo@uptc.edu.co (M.H.B.)
 - ² Grupo de Investigación en Gestión Administrativa y Empresarial Sostenible (GIGAS), Universidad Pedagógica y Tecnológica de Colombia UPTC, Avenida Central del Norte, Boyacá, Tunja 150003, Colombia
 - ³ Instituto de Ciencia de Materiales de Sevilla (ICMS), Centro Mixto Universidad de Sevilla-CSIC, Américo Vespucio 49, 41092 Seville, Spain; andresno959@gmail.com (A.N.M.-G.); pscb14495@yahoo.es (P.S.-C.); navio@us.es (J.A.N.); carmen.hidalgo@csic.es (M.C.H.)
 - ⁴ Departamento de Química, Universidad de Tolima, Barrio Santa Elena, Ibagué 730005, Colombia
- * Correspondence: cajaramillopa@ut.edu.co

Abstract: Different composites based on ZnO/Ag₃PO₄ and ZnO–malachite (Cu₂(OH)₂CO₃) were synthesized in order to determine their effectiveness in the treatment of municipal and industrial wastewaters (mainly polluted by enteropathogenic bacteria, dyes, and heavy metals). The addition of Ag₃PO₄ and malachite did not significantly modify the physicochemical properties of ZnO; however, the optical properties of this oxide were modified as a result of its coupling with the modifiers. The modification of ZnO led to an improvement in its effectiveness in the treatment of municipal and industrial wastewater. In general, the amount of malachite or silver phosphate and the effluent to be treated were the determining factors in the effectiveness of the wastewater treatment. The highest degree of elimination of bacteria from municipal wastewater and discoloration of textile staining wastewater were achieved by using ZnO/Ag₃PO₄ (5%), but an increase in the phosphate content had a detrimental effect on the treatment. Likewise, the highest Fe and Cu photoreduction from coal mining wastewater was observed by using ZnO–malachite (2.5%) and ZnO/Ag₃PO₄ (10%), respectively. Some of the results of this work were presented at the fourth Congreso Colombiano de Procesos Avanzados de Oxidación (4CCPAOX).

Keywords: municipal effluents; textile staining wastewater; coal mining drainages; photocatalysis; ZnO(-malachite-Ag₃PO₄)

1. Introduction

Municipal effluents, textile staining wastewater, and coal mining wastewater currently represent important pollution problems in Latin-American countries. A clear example of this reality can be found in Colombia, where municipal and industrial wastewaters have a detrimental effect on the quality of natural water sources that significantly impacts animal and human health.

Different techniques for contaminant removal from wastewater have been evaluated around the world [1]. Adsorbents are the main materials employed for the removal of dyes and heavy metals. These materials present excellent performance; however, by using adsorption, the pollutants are transferred to a new phase, so this treatment is not a

definitive solution for the environmental problem represented by the abovementioned contaminants [2]. Ozonization has also been successfully improved for water purification [3]; however, this process is only effective for the degradation of organic compounds, and heavy metals still remain in the liquid phase.

Combinations of advanced oxidation processes (AOPs) have also been studied for the treatment of organic pollutants. For example, D. Yu et al. have deeply studied combinations of AOPs. They have reported the successful degradation and mineralization of 4-nitrophenol (4-NP) by using photocatalysis combined with ozonation and Fe-based metal–organic frameworks (MOFs) [4]. These authors have also reported the degradation of 4-NP by using Fenton-like processes based on Fe-MOFs [5]. Tetracycline (TC) degradation has also been successfully performed by different authors. For example, O. Alani et al. have reported the treatment of this compound with a heterogeneous photo-Fenton process based on bio-templated $\text{Fe}_3\text{O}_4/\text{CuO}/\text{C}$ [6]. On the other hand, H. Ari et al. [7] have combined a UV-assisted Fenton process with nanostructured biomimetic $\alpha\text{-Fe}_2\text{O}_3$, thus showing efficient UV–Fenton degradation for TC. This catalyst can also be reused in up to five consecutive cycles without a significant loss in activity.

The current research simultaneously addresses the serious environmental problems represented by enteropathogenic bacteria, dyestuffs, and heavy metals by means of photocatalytic processes. In this study, different composites based on ZnO and modified with the addition of Ag_3PO_4 or $\text{Cu}_2(\text{OH})_2\text{CO}_3$ were tested in the photocatalytic treatment of real effluents from domestic and industrial activities. The evaluated photocatalysts were found to be very effective at eliminating pollutants from the tested wastewaters and improve on the efficiency of the photocatalysts that our research group studied previously [8–12].

The main objective of this study was to improve ZnO's photoactivity by modifying it with $\text{ZnO}/\text{Ag}_3\text{PO}_4$ and $\text{ZnO}-\text{Cu}_2(\text{OH})_2\text{CO}_3$ and evaluating the effects of these composites in real wastewater samples. Authors have reported that Ag_3PO_4 can help ZnO improve its optical response in the visible region of the electromagnetic spectrum [13,14]. Likewise, it has also been reported that malachite ($\text{Cu}_2\text{CO}_3(\text{OH})_2$) is an effective modifier of TiO_2 , leading to an improvement in the effectiveness of this semiconductor in photocatalytic hydrogen production [15].

In the current study, the efficiency of ZnO modified by Ag_3PO_4 or $\text{Cu}_2\text{CO}_3(\text{OH})_2$ addition was studied in the treatment of wastewater by photocatalysis. This research makes a beneficial contribution to the use of photocatalysis to treat real wastewaters, such as municipal, handicraft factory, and coal mining effluents.

2. Materials and Methods

2.1. $\text{ZnO}/\text{Ag}_3\text{PO}_4$ and ZnO –Malachite Preparation

Pure ZnO was prepared by mixing two aqueous solutions of $\text{Zn}(\text{CH}_3\text{COO})_2 \cdot 2\text{H}_2\text{O}$ (Sigma-Aldrich, $\geq 99.0\%$ purity) and Na_2CO_3 (Panreac, 99.0% purity) in stoichiometric proportions. After 2 h of mixing, the obtained powders were filtered, dried, and heated to 400 °C for 2 h.

$\text{ZnO}/\text{Ag}_3\text{PO}_4$ composites were prepared by following the procedure previously reported by J.A Navío et al. [14]. The ZnO powders were briefly suspended under continuous stirring in a Na_3PO_4 (Sigma–Aldrich, $<96\%$) water solution. Then, a solution of AgNO_3 (Sigma–Aldrich, 99.8%) was dropped into the suspension and after stirring for 30 min the solid was recovered by centrifugation. The nominal molar percentages of Ag_3PO_4 selected for this study were 5%, 10%, and 50%. These materials were labeled $\text{ZnO}/\text{Ag}_3\text{PO}_4$ (5%), $\text{ZnO}/\text{Ag}_3\text{PO}_4$ (10%), and $\text{ZnO}/\text{Ag}_3\text{PO}_4$ (50%), respectively.

ZnO –malachite composites were prepared by the dispersion of the pure ZnO obtained previously in an aqueous solution of CuSO_4 under continuous stirring for 1 h. Afterwards, an aqueous solution of Na_2CO_3 was added drop by drop in amounts such to obtain nominal malachite contents of 0.5% and 2.5% (molar percentages). These materials were labeled $\text{ZnO}-\text{M}$ (0.5%) and $\text{ZnO}-\text{M}$ (2.5%), respectively.

2.2. Physicochemical Properties Analysis

The physicochemical properties of the composites were evaluated by using different analytical techniques and pieces of equipment, which are described below.

The chemical composition of the materials was estimated by X-ray fluorescence (XRF). Measurements were performed on pressed pellets in which samples were fixed in 10 wt.% wax. The analyses used a Panalytical Axios sequential spectrophotometer equipped with a Rh tube as the source of radiation.

BET specific surface areas were determined by N₂ adsorption at 77 K in a Micromeritics ASAP 2010 instrument. Degassing of the samples was performed at 150 °C for 30 min under a helium flow.

UV-Vis diffuse reflectance spectrophotometry was used to study the optical properties of the materials. Spectra were recorded in the range between 200 nm and 800 nm in absorption mode using a Varian spectrometer (model: Cary100) equipped with an integrating sphere and using BaSO₄ as a 100% absorption reference material. Band-gap values were calculated from the Kubelka–Munk functions $F(R_{\infty})$, which are proportional to the absorption of radiation, by plotting $(F(R_{\infty}) \times hu)^{1/2}$ against hu .

X-ray diffraction analyses used a X' PertPro PANalytical instrument equipped with a Cu K α 1 radiation source ($\lambda = 0.15406$ nm) (45 kV, 40 mA). The 2θ range was between 10° and 80°. A step size of 0.05° and a step time of 80 s were used.

Finally, the morphology of the samples was observed using scanning electron microscopy (SEM) in a Hitachi S 4800 microscope and by transmission scanning microscopy (S/TEM) in a Talos™ F200S FEI microscope.

2.3. Wastewater Sampling

The water samples selected for this study corresponded to municipal and industrial wastewater from three different sources. Water samples from three Colombian towns highly influenced by domestic and industrial activities were included in this study. Firstly, municipal wastewater was collected from a highly polluted river in the city of Tunja (geographical coordinates: Latitude: 5.553583; Longitude: −73.350694). Handmade textile wastewater was also obtained at the exit of the staining tanks of factories located in the town of Nobsa (Latitude: 5.77333; Longitude: −72.94833). Finally, coal mining wastewater was taken from the town of Samacá (Latitude: 5.49444, Longitude: −73.48833). The wastewater samples were collected by following the procedure described in the Standard Methods for Examination of Water and Wastewater (SMEWW) [16].

2.4. Photocatalytic Wastewater Treatment

ZnO nanocomposites were prepared according to the methods described in Section 2.1 and were tested in the photocatalytic treatment of the municipal and industrial wastewater samples. A detailed description of the procedure employed in each of the photocatalytic tests conducted is presented below.

All the experiments were carried out twice in a 400 mL Pyrex reactor wrapped in aluminum foil with a 250 mL sample of wastewater and 1 g/L of photocatalyst loading. A total reaction time of 240 min was used along with an Osram Ultra-Vitalux lamp (300 W) as the light source with a sun-like radiation spectrum, a UVA range at 365 nm, and an intensity of 30 W/m². The adsorption–desorption equilibrium was achieved by stirring for 10 min in the dark before switching on the lamp. Magnetic stirring and a constant natural oxygen flow of 35 L/h coming from a bubbler tank were maintained throughout the photocatalytic treatment time. Photocatalyst recovery was carried out by filtration with Sartorius Biolab filters with a pore size of 0.45 μ m. Photolysis tests (without photocatalyst) were also carried out.

A complete physicochemical analysis of the wastewater samples before and after treatment was carried out by double testing. These measurements included pH, alkalinity, and chloride content determination. The pH was measured with an SI analytics Lab

850 pH-meter. Alkalinity and chloride content were calculated by using the 2320 B-1995 APHA and 4500 Cl-B-1995 APHA methods, respectively [16].

Total organic carbon (TOC) was also determined by using a TOC/TN analyzer (multi N/C 2100 Analytik Jena). Method 5310B from the SMEWW was employed [16].

In order to evaluate the effectiveness of the treatment in the removal of enteropathogenic bacteria from municipal and handmade textile factory wastewater, all samples were analyzed before and after the photocatalytic reaction by using the Merck membrane filtration method (method 9222) [16]. Coliforms Chromocult® agar was used as the culture medium. The results obtained are reported as colony forming units (CFU)/100 mL of wastewater sample.

In the case of the stained wastewater from the textile factories, discoloration was also analyzed by UV-Vis spectrophotometry with a Thermo Scientific Evolution 300 spectrophotometer. The main absorption signal presented in these effluents was observed at 450 nm. Samples were collected after 30, 60, 120, 180, and 240 min. The percentage of discoloration was calculated by using Equation (1).

$$\text{Discoloration (\%)} = ((A - B)/A) \times 100 \quad (1)$$

where:

A = absorbance value of the starting sample at 450 nm; and

B = absorbance value of the sample after a determined reaction time.

Considering the complex composition of the coal mining wastewater samples, only photocatalysts showing promising results in the treatment of municipal and stained wastewater were selected to be evaluated in the treatment of the acidic mining drainage. In this case, the effectiveness of the photocatalysts employed was determined by the removal of heavy metals. Thus, the concentration of these pollutants was evaluated using atomic absorption spectroscopy in a Shimadzu AA-7000 spectrophotometer. All samples (from the liquid phase or solid catalysts) were subjected to acidic digestion by the addition of 3 mL of HNO₃ (c) at 180 °C for 30 min (method 3010 from the SMEWW) [16].

In order to ensure the reproducibility and reliability of the obtained results, selected photocatalytic reactions and all of the physicochemical analyses were carried out twice. Herein, we report the values from the arithmetic average obtained for all the results, and the standard deviation was also calculated.

3. Results and Discussion

3.1. Characterization of the ZnO-Based Composites

Compositional, structural, and spectroscopic analysis of the ZnO/Ag₃PO₄ and ZnO-malachite composites showed the different properties of the photocatalysts. The results for ZnO/Ag₃PO₄ have been previously reported [14]; therefore, the current study provides only an overview.

As shown in Table 1, the chemical composition of the analyzed materials determined by XRF agrees with the theoretical values, thus indicating a good incorporation of Ag₃PO₄ and Cu₂(OH)₂CO₃ in the ZnO matrix. Table 1 also shows the specific surface area values for all the samples. The value for ZnO is 30.20 m²/g and decreases with the incorporation of Ag₃PO₄ and malachite in the composites due to the much lower surface area of the phosphate and malachite (2.7 m²/g in both cases). This effect is more evident as the phosphate content increases; the surface area of the composite with 50% phosphate addition decreased to 17.27 m²/g. N₂ adsorption-desorption curves are presented as supplementary material in Figures S1 and S2. As can be seen in these figures, no significant differences were observed after Ag₃PO₄ or malachite incorporation into the ZnO matrix. However, it is evident that all materials present a type III isotherm with the H1 hysteresis loop [17], and the behavior of the N₂ adsorption-desorption isotherms is the same regardless of the type and amount of dopant used.

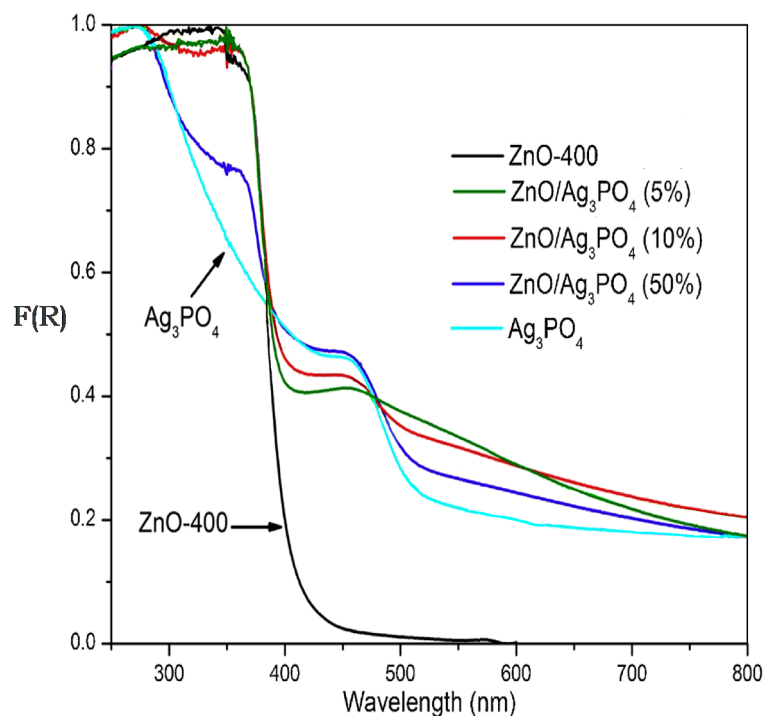
Table 1. Summary of characterization results.

Photocatalyst	XRF (%)					S_{BET} (m ² /g)	Band Gap (eV)
	Zn	O	Ag	P	Cu		
ZnO	ND *	ND *	—	—	—	30.20	3.25
Ag ₃ PO ₄	—	14.82	78.21	6.97	—	2.73	2.43
Malachite	—	—	—	—	ND	2.70	ND
ZnO/Ag ₃ PO ₄ (5%)	66.95	18.26	13.33	1.45	—	28.62	1.90
ZnO/Ag ₃ PO ₄ (10%)	56.76	18.54	22.42	2.28	—	26.53	2.26
ZnO/Ag ₃ PO ₄ (50%)	27.32	16.85	50.91	4.93	—	17.27	2.40
ZnO-M (0.5%)	79.43	19.98	—	—	0.59	27.60	ND
ZnO-M (2.5%)	75.00	21.86	—	—	3.14	29.50	ND

* ND = There is no determined.

The band-gap values for selected composites were determined by UV-Vis DRS spectrophotometry (Table 1). It can be observed that after the coupling of ZnO and Ag₃PO₄, the ZnO band-gap value decreased. It is worth noting that the lowest value was obtained with the addition of less Ag₃PO₄ (5%); the value then increased as the phosphate content increased.

Figure 1 shows the UV-Vis DR spectra for ZnO and the composites. In this figure, the absorption for ZnO, Ag₃PO₄, and malachite located between 200 and 450 nm is very high. When ZnO was coupled with the modifying agents, its absorption increased significantly in the visible region of the electromagnetic spectrum. This absorption in the visible region increased as the Ag₃PO₄ or malachite content increased. Regarding the ZnO-M materials, no significant differences were observed with DRS, which may be because malachite is found in low concentrations in ZnO. A high absorption shoulder was observed in the visible range, which may be indicative of the presence of this material because the spectrum of the precursor material also presents a high absorption value in the visible range. This characteristic can be assigned to the Cu(II) d–d transition [18].

**Figure 1.** Cont.

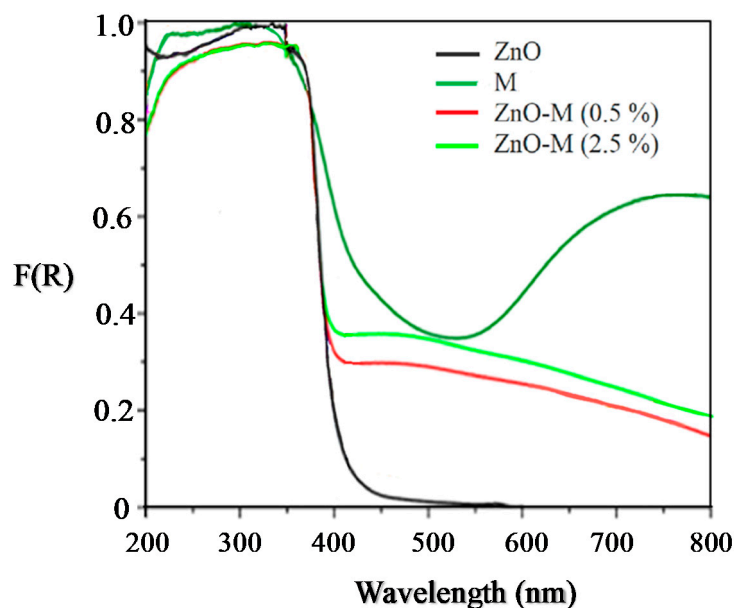


Figure 1. UV-Vis DR spectra for the ZnO/Ag₃PO₄ (up) and ZnO-M (down) composites.

XRD patterns of the different samples are depicted in Figure 2. For the ZnO/Ag₃PO₄ composites (Figure 2a), the characteristic peaks for Ag₃PO₄ and ZnO can be observed with a cubic phase and Wurtzite structure, respectively. The increase in Ag₃PO₄ content leads to a gradual increase in the intensity of the signal (200) corresponding to phosphate, while the intensity of the signals for ZnO decreases.

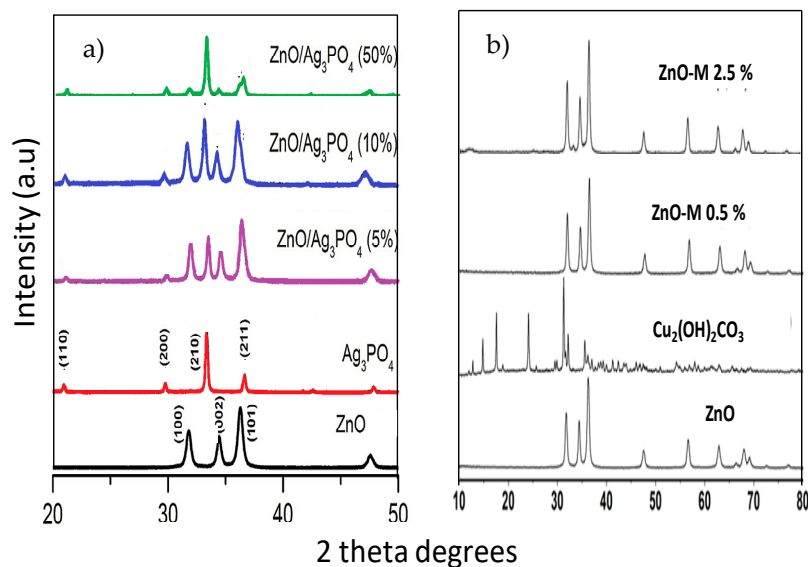


Figure 2. (a) X-ray diffraction patterns for the ZnO/Ag₃PO₄ and (b) ZnO–malachite composites.

Figure 2b. depicts the diffractograms for ZnO–malachite composites. Only peaks corresponding to ZnO Wurtzite can be observed. Even for the sample with the highest malachite content, no peaks associated with this mineral can be seen. This is probably due to the low amount and good dispersion of malachite on the ZnO matrix; however, the XRF results show that in the ZnO-M materials there are different Cu concentrations, which are dependent on the nominal amount added during synthesis.

The morphology and composition of the studied materials were analyzed by SEM and selected images are presented in Figures 3 and 4. As can be seen in Figure 3, Ag₃PO₄ is heterogeneously dispersed in ZnO/Ag₃PO₄ (5%) and ZnO/Ag₃PO₄ (10%). On the

other side, the ZnO/Ag₃PO₄ (50%) material is present as a homogeneous dispersion of aggregates with a diameter of 50 nm on the ZnO particles (25 nm).

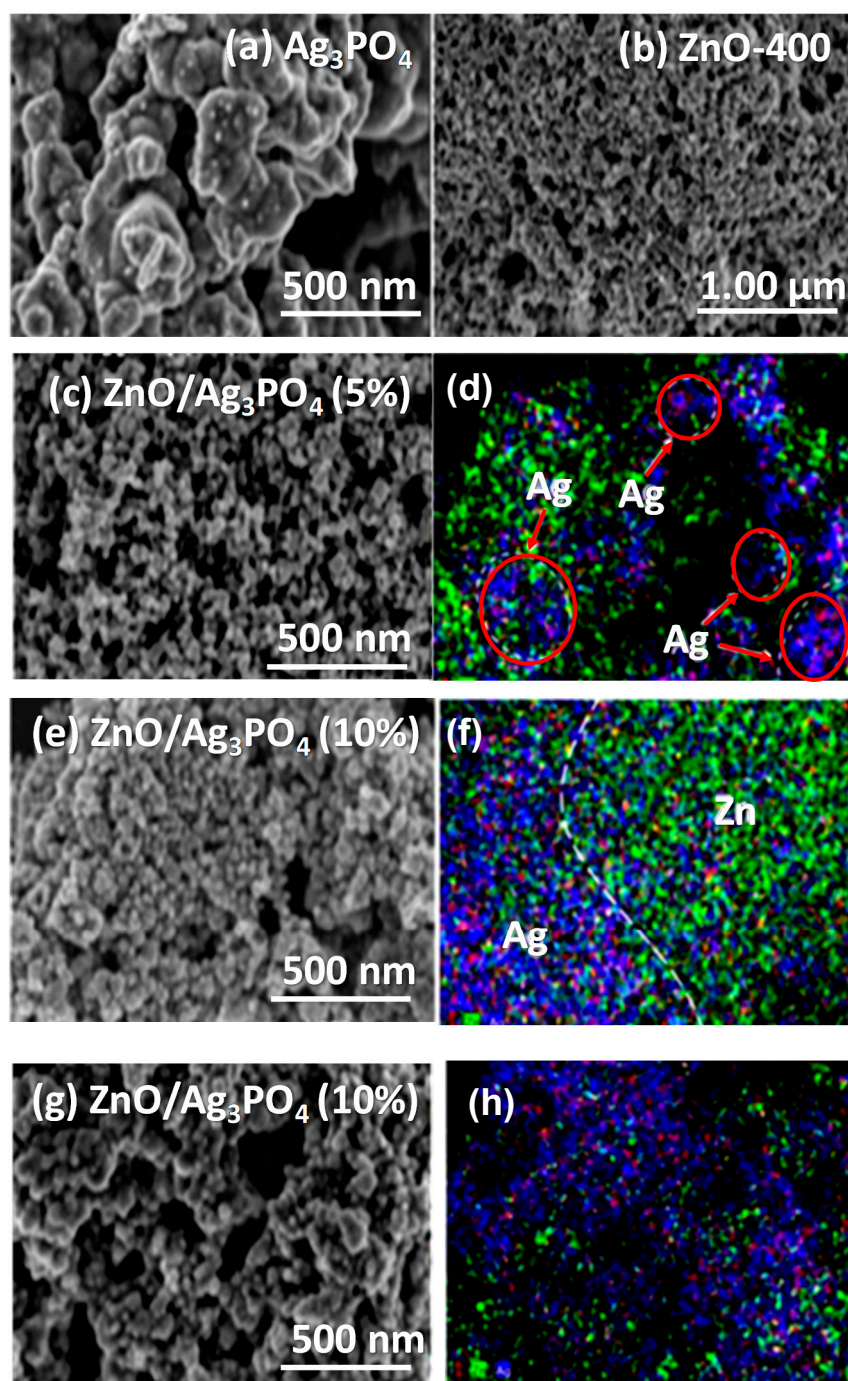


Figure 3. SEM images of ZnO/Ag₃PO₄ composites. (a) Ag₃PO₄; (b) ZnO-400; (c) and (d) ZnO/Ag₃PO₄ (5%); (e) and (f) ZnO/Ag₃PO₄ (10%); and (g) and (h) ZnO/Ag₃PO₄ (10%).

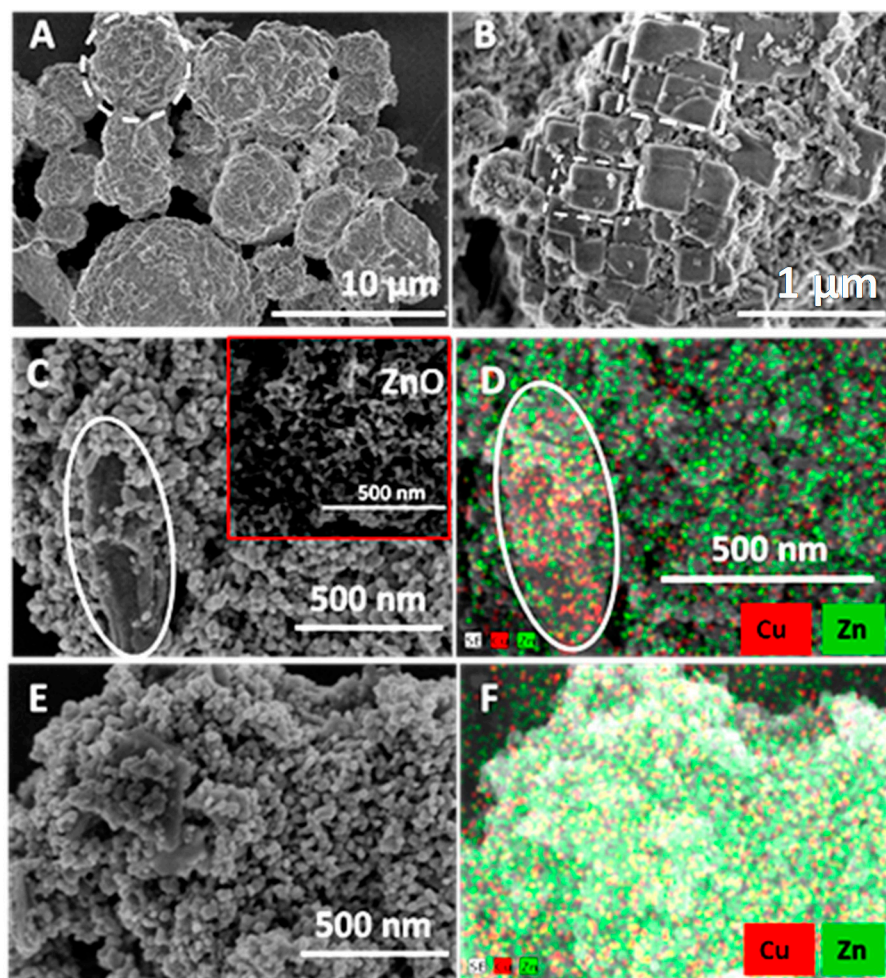


Figure 4. SEM images of ZnO-M composites. (A,B) $\text{Cu}_2\text{CO}_3(\text{OH})_2$; (C,D) ZnO-M (0.5%); (E,F) ZnO-M (2.5%).

Figure 4 shows images of ZnO-M composites. Here, it is possible to identify ZnO particles with a shape like rice grains. In the case of malachite, the morphology of this mineral is more regular with round structures and a flower shape.

3.2. Photocatalytic Wastewater Treatment

3.2.1. Municipal Wastewater

Citrobacter spp., *E. coli*, *Salmonella* sp., and coliforms were the main species of bacteria present in the studied municipal wastewater samples (samples taken from a river). During the photocatalytic tests, samples from the reactor were taken at different times: 30, 60, 120, 180, and 240 min. For all the photocatalysts tested, the number of bacteria of all of these species decreased as the photoreaction time increased.

The results obtained from the removal of bacteria after 240 min of photocatalytic treatment are presented in Table 2. As expected, the bacteria were sensitive to UV-Vis light, leading to a decrease in their number during the photolysis tests performed under illumination without a catalyst.

Table 2. Enteropathogenic bacteria removed from a river water sample highly polluted with municipal wastewater.

Photocatalytic Removal Test	<i>Citrobacter</i> spp. *	<i>E. coli</i> *	<i>Salmonella</i> sp.*	Other Coliforms *	Total (UCF)	Elimination (%)
Starting sample	500	4000	2500	7800	14,800	0
Photolysis	400	3540	1800	6200	11,940	16.5
ZnO	300	800	1200	3200	5500	61.5
Malachite	400	1000	800	3600	5800	59.4
ZnO-M (0.5%)	10	0	300	510	820	94.3
ZnO-M (2.5%)	0	0	200	250	450	96.8
Ag ₃ PO ₄	100	100	100	200	500	96.5
ZnO/Ag ₃ PO ₄ (5%)	0	0	2	0	2	99.9
ZnO/Ag ₃ PO ₄ (10%)	0	20	200	120	340	97.6
ZnO/Ag ₃ PO ₄ (50%)	0	10	50	185	245	98.3

* These results are expressed as UCF of enteropathogenic bacteria.

When ZnO or any of the composites were added to the reactor, the elimination of bacteria increased significantly, thus showing the bactericidal effect of the photocatalytic process. This effect is mainly caused by the generation of radical oxygen species, which are responsible for the breakup of the plasma membrane [19–21]. Malachite was also observed to be less effective than ZnO in the elimination of coliforms, but it also had a bactericidal effect conferred by the presence of Cu in its structure.

In order to improve the photocatalytic performance of ZnO, this semiconductor was combined with malachite. The addition of 2.5% of malachite resulted in the complete elimination of *Citrobacter* spp. and *E. coli* after 240 min of treatment; however, other species were still detected in the sample. In both cases, malachite can act as an electron sink that can facilitate charge transfer, leading to a better gap–electron separation [15].

It can also be observed that in the ZnO-M materials there is a synergistic effect between the zinc oxide and the malachite in the elimination of bacteria that is directly proportional to the malachite content. This significantly exceeds the effect caused by the bare materials.

Ag₃PO₄ was also tested as a modifying agent for ZnO as shown in Table 2. This compound is more effective in the removal of bacteria than ZnO and malachite. As a result, the ZnO–Ag₃PO₄ combination significantly improves the effectiveness of the semiconductor in the elimination of bacteria. The complete elimination of all enteropathogenic species from the municipal wastewater was achieved after 300 min of total reaction time by using the photocatalyst prepared by the addition of 5% of Ag₃PO₄ to ZnO (i.e., ZnO/Ag₃PO₄ (5%)).

An increase in the content of Ag₃PO₄ above 5% had a detrimental effect on the photocatalytic activity of ZnO, which may have been due to the possible obstruction of active sites on the ZnO surface.

Besides the microbiological analysis, a complete physicochemical analysis of the wastewater samples was also carried out. A comparative presentation of the TOC analysis results is included in Figure 5. As shown in the figure, the highest TOC removal value was achieved by using the photocatalyst labeled ZnO/Ag₃PO₄ (5%), with a final TOC value of 6.5 mg/L.

Parameters such as pH, alkalinity, hardness, and chloride content, which are presented in Table 3, remained almost constant after the photocatalytic treatment. These results show that photocatalytic phenomena have priority over the adsorption processes for ionic species, such as chlorides and carbonates, on the photocatalysts' surface.

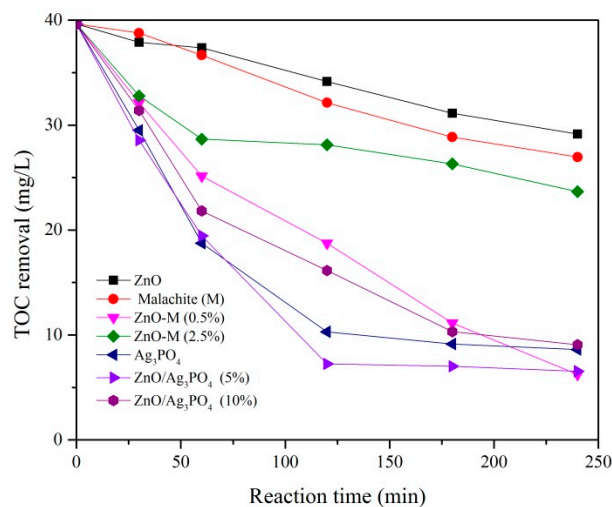


Figure 5. Total organic carbon content in the municipal wastewater samples before and after treatment.

Table 3. Analysis of physicochemical parameters before and after photocatalytic treatment of municipal and handmade textile staining wastewater.

Photocatalyst	Reaction Time (Min)	Hardness (Mg/L CaCO ₃)	Alkalinity (Mg/L CaCO ₃)	Chloride Content (Mg/L Cl ⁻)	pH
Municipal Wastewater					
Photolysis	0	115	375.33	1181.8	6.35
	240	100	350.30	1063.6	6.39
ZnO	0	120	375.33	1299.9	6.5
	240	115	350.30	1063.6	6.08
ZnO-M (0.5%)	0	130	400.35	1299.9	6.19
	240	115	375.33	1181.8	6.58
ZnO-M (2.5%)	0	120	425.37	1299.9	6.62
	240	105	375.33	1063.6	6.34
Malachite	0	120	400.35	1181.8	6.46
	240	120	325.28	1181.8	6.39
Ag ₃ PO ₄	0	130	375.33	1418.1	6.57
	240	120	375.33	1299.9	6.14
ZnO/Ag ₃ PO ₄ (5%)	0	125	425.37	1063.6	6.82
	240	115	400.35	945.41	6.79
ZnO/Ag ₃ PO ₄ (10%)	0	130	425.37	1299.9	6.65
	240	120	375.33	1181.8	6.64
ZnO/Ag ₃ PO ₄ (50%)	0	120	400.35	1299.9	6.32
	240	115	350.30	1063.6	6.42
Handmade Textile Staining Wastewater					
Photolysis	0	1065	700.61	8390.5	4.61
	240	1065	675.59	8390.5	4.61
ZnO	0	1060	675.58	8508.7	4.61
	240	1060	575.49	8508.7	5.86
ZnO-M (0.5%)	0	1055	725.63	8863.3	4.69
	240	1045	675.59	8626.9	5.1
ZnO-M (2.5%)	0	1030	675.59	8508.7	4.81
	240	1045	675.59	7917.8	4.93
Malachite	0	1080	725.63	8508.7	4.64
	240	1035	675.59	8508.7	4.87
Ag ₃ PO ₄	0	1055	725.63	8390.5	4.58
	240	1070	675.59	8272.4	4.60
ZnO/Ag ₃ PO ₄ (5%)	0	1060	700.61	8626.9	4.81
	240	1055	650.56	8036	5.03
ZnO/Ag ₃ PO ₄ (10%)	0	1060	700.61	8745.1	4.7
	240	1045	675.59	8508.7	5.29
ZnO/Ag ₃ PO ₄ (50%)	0	1080	725.63	8626.9	4.71
	240	1065	700.61	8508.7	5.38

3.2.2. Handmade Textile Factory Wastewater

Citrobacter spp. were not detected in the handmade textile staining wastewater samples. For the rest of studied bacteria species, a similar behavior to that observed in the municipal wastewater treatment was found (Section 3.2.1); i.e., it was also determined that the highest bactericidal efficiency was obtained by using ZnO/Ag₃PO₄ (5%) as a photocatalyst (Table 4).

Table 4. Enteropathogenic bacteria removal from samples of handmade textile staining wastewater.

Photocatalytic Removal Test	<i>E. coli</i> *	<i>Salmonella</i> sp. *	Other Coliforms *	Total (UCF)	Elimination (%)
Starting sample	1460	390	1850	3700	0
Photolysis	1320	350	1670	3340	9.7
ZnO	80	40	120	240	93.5
Malachite (M)	30	250	540	820	77.8
ZnO-M (0.5%)	50	25	85	160	95.7
ZnO-M (2.5%)	35	20	45	100	97.3
Ag ₃ PO ₄	30	10	0	40	98.9
ZnO/Ag ₃ PO ₄ (5%)	0	1	0	1	99.9
ZnO/Ag ₃ PO ₄ (10%)	0	20	23	43	98.8
ZnO/Ag ₃ PO ₄ (50%)	10	30	50	90	97.6

* These results are expressed as UCF of enteropathogenic bacteria.

The addition of malachite to ZnO increased the effectiveness of ZnO in removing bacteria. The sample with 2.5% of malachite was the best photocatalyst in this series. The addition of Ag₃PO₄ also considerably increased the effectiveness of ZnO in removing bacteria. This resulted in the sample with the lowest content of phosphate (5%) being the one with the best photocatalytic activity. An increase in the silver phosphate content had a detrimental effect on the overall effectiveness of the photocatalytic treatment, probably due to a screening effect of the phosphate on the surface-active sites of ZnO.

On the other hand, the TOC analyses (Figure 6) showed that the handmade textile staining effluents had a higher TOC content than that observed in the municipal wastewater samples due to the high content of organic dyestuffs present in these effluents. In this case, ZnO/Ag₃PO₄ (10%) yielded the lowest TOC value after 240 min of treatment; however, all photocatalytic tests achieved TOC values lower than 800 mg/L.

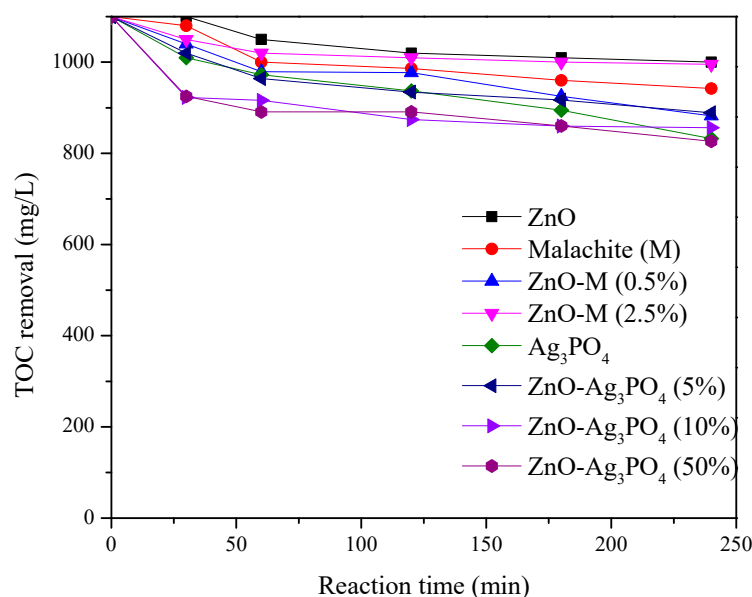


Figure 6. Total organic carbon content in handmade textile staining wastewater samples.

Photodegradation of dyestuffs in the handmade textile staining wastewater samples during the photocatalytic treatment was evaluated by measuring the percentage of discoloration after the treatment (Table 5). The highest dyestuffs removal value (73.63%) was obtained by using the ZnO/Ag₃PO₄ (5%) photocatalyst. This result is consistent with the TOC analysis results (Figure 6).

Table 5. Discoloration of the handmade textile staining wastewater samples after 240 min of photocatalytic treatment.

Photocatalytic Test	Discoloration (%)	Standard Deviation (SD)
Photolysis	11.85	1.31
ZnO	67.33	2.05
Malachite (M)	52.86	0.83
ZnO-M (0.5%)	70.46	0.45
ZnO-M (2.5%)	69.90	0.15
Ag ₃ PO ₄	62.86	1.58
ZnO/Ag ₃ PO ₄ (5%)	73.63	1.75
ZnO/Ag ₃ PO ₄ (10%)	69.43	0.90
ZnO/Ag ₃ PO ₄ (50%)	70.96	0.66

3.2.3. Coal Mining Wastewater

The acid mining drainage (AMD) evaluated in this study was primarily composed of iron and copper. Other metals were not detected in the analyzed samples; however, they could be present in amounts lower than the detection limit of the atomic absorption spectroscopy technique.

The Fe and Cu concentrations present in the AMD before and after photocatalytic treatment using ZnO and the composite catalysts are reported in Table 6. The Colombian regulations indicate a maximum amount of 2 mg/L of total iron in AMD; however, as shown in this table, the content of this metal significantly exceeds the maximum level (9 mg/L). For this reason, it is very important to find strategies for the treatment of AMD that are focused on the removal of the metals in these effluents before they are poured into the drain or natural water sources.

Table 6. Iron and copper removal from coal mining wastewater after 120 min of photocatalytic treatment.

Photocatalytic Test	Main Metals in the Liquid Phase	
	Fe (ppm)	Cu (ppm)
Starting sample	9.00	0.20
Blank test	3.21	0.18
ZnO	2.01	-
Malachite (M)	2.20	-
ZnO-M (0.5%)	1.70	-
ZnO-M (2.5%)	1.20	0.13
Ag ₃ PO ₄	2.20	-
ZnO/Ag ₃ PO ₄ (5%)	2.10	-
ZnO/Ag ₃ PO ₄ (10%)	1.24	0.08
ZnO/Ag ₃ PO ₄ (50%)	2.47	-

According to Colombia's national regulations for Cu content in AMD, the maximum permissible level is 1 mg/L. In the studied samples, the value of this parameter was under the maximum value (0.20 mg/L); however, it is also important to try to decrease the content of this metal in the wastewater.

Table 6 shows the degree of iron and copper removal from the coal mine wastewater after 120 min of photocatalytic treatment using the different photocatalysts. Metals present in the wastewater, such as Cu and iron, can be photocatalytically reduced on the catalyst's surface [9,22–26] and thus removed from the water. The catalysts were analyzed after

each reaction, and it was found that the content of metals removed from the liquid phase passed to the catalyst's surface. The photocatalyst ZnO/Ag₃PO₄ (10%) had estimated concentrations of Fe and Cu of 6.43 mg/L and 0.08 mg/mL, respectively. On the other hand, ZnO-M (2.5%) had an Fe concentration of 6.39 mg/mL and no result was obtained for Cu since it was below the limit of detection using this technique.

The highest Fe and Cu removal value was achieved by using ZnO-M (2.5%) and ZnO/Ag₃PO₄ (10%). With these materials, it was possible to decrease the Fe and Cu content in the liquid phase to values lower than those permitted by Colombian regulations. As can also be seen in Table 6, the iron content decreased during the blank test (under UV-Vis light and without photocatalyst). This may have been due to the reduction of this metal on the reactor's surface as evidenced by the change in the color of that element after the photoreaction. In the case of Cu, the reduction in the metal content was negligible.

4. Conclusions

Enteropathogenic bacteria, dyestuffs, and metals were detected in the municipal and industrial wastewater studied and their removal was attempted by photocatalytic treatment using ZnO and ZnO-malachite and ZnO/Ag₃PO₄ composites.

In order to improve the effectiveness of the photocatalytic treatment, ZnO was modified by the addition of different concentrations of silver phosphate and malachite. Using physicochemical characterization, it was possible to observe that the addition of these compounds did not significantly change the starting properties of the zinc oxide. However, the addition of phosphate or malachite to ZnO considerably improved its photocatalytic efficiency in the overall effectiveness of the treatment.

In general, throughout all the photocatalytic tests performed, the greatest effectiveness in the removal of pollutants (bacteria, dyestuffs, and metals) was achieved by using the ZnO/Ag₃PO₄ (5%) and ZnO-malachite (2.5%) composites. This led to final values of contaminants within the values allowed by Colombian regulations for treated waters. As a consequence of these results, the photocatalysts studied could allow for wastewater to be recycled for uses such as irrigation and industrial activities according to the amounts of enteropathogenic bacteria, discoloration levels, and Fe and Cu concentrations. Further studies remain necessary to gain a deeper understanding of all the parameters considered in Colombia's regulations.

Supplementary Materials: The following are available online at <https://www.mdpi.com/article/10.3390/w13162264/s1>, Figure S1, N₂ adsorption-desorption isotherms for ZnO-malachite composites; Figure S2, N₂ adsorption-desorption isotherms for ZnO/Ag₃PO₄ composites.

Author Contributions: Conceptualization, Methodology, Supervision, and Funding acquisition, J.J.M.; Investigation, J.S.H.N., A.N.M.-G., and P.S.-C.; Project administration, H.R.; writing—original draft preparation, M.C.H. and C.J.-P.; writing—review and editing, J.A.N. and M.H.B. All authors have read and agreed to the published version of the manuscript.

Funding: This research was funded by Gobernación de Boyacá from the Fondo Nacional de Financiamiento para la Ciencia, la Tecnología e Innovación (Project 789-2020) and from the Universidad Pedagógica y Tecnológica de Colombia Projects SGI 3007, 2644, and 2804.

Institutional Review Board Statement: Not applicable.

Informed Consent Statement: Not applicable.

Data Availability Statement: Not applicable.

Acknowledgments: This work was financed with resources from the Gobernación de Boyacá from the Fondo Nacional de Financiamiento para la Ciencia, la Tecnología e Innovación (Project 789-2020) and from the Universidad Pedagógica y Tecnológica de Colombia Projects SGI 3007, 2644, and 2804.

Conflicts of Interest: The authors declare no conflict of interest.

References

1. Luo, J.; Yu, D.; Hristovski, K.D.; Fu, K.; Shen, Y.; Westerhoff, P.; Crittenden, J.C. Critical Review of Advances in Engineering Nanomaterial Adsorbents for Metal Removal and Recovery from Water: Mechanism Identification and Engineering Design. *Environ. Sci. Technol.* **2021**, *55*, 4287–4304. [CrossRef]
2. Yu, D.; Wang, Y.; Wu, M.; Zhang, L.; Wang, L.; Ni, H. Surface functionalization of cellulose with hyperbranched polyamide for efficient adsorption of organic dyes and heavy metals. *J. Clean. Prod.* **2019**, *232*, 774–783. [CrossRef]
3. Yu, D.; Wang, L.; Yang, T.; Yang, G.; Wang, D.; Ni, H.; Wu, M. Tuning Lewis acidity of iron-based metal-organic frameworks for enhanced catalytic ozonation. *Chem. Eng. J.* **2021**, *404*, 127075. [CrossRef]
4. Yu, D.; Lia, L.; Wua, M.; Crittenden, J.C. Enhanced photocatalytic ozonation of organic pollutants using an iron based metal-organic framework. *Appl. Catal. B* **2019**, *251*, 66–75. [CrossRef]
5. Yang, T.; Yu, D.; Wang, D.; Yang, T.; Li, Z.; Wu, M.; Petru, M.; Crittenden, J. Accelerating Fe(III)/Fe(II) cycle via Fe(II) substitution for enhancing Fenton-like performance of Fe-MOFs. *Appl. Catal. B* **2021**, *286*, 119859. [CrossRef]
6. Alani, O.A.; Ari, H.A.; Alani, S.O.; Offiong, N.-A.O.; Feng, W. Visible-Light-Driven Bio-Templated Magnetic Copper Oxide Composite for Heterogeneous Photo-Fenton Degradation of Tetracycline. *Water* **2021**, *13*, 1918. [CrossRef]
7. Ari, H.A.; Alani, O.A.; Zeng, Q.-R.; Ugya, Y.A.; Offiong, N.-A.O.; Feng, W. Enhanced UV-assisted Fenton performance of nanostructured biomimetic α -Fe₂O₃ on degradation of tetracycline. *J. Nanostruct. Chem.* **2021**. Available online: [https://link-springer-com.ezproxy.javeriana.edu.co/search?query=Enhanced+UV-assisted+Fenton+performance+of+nanostructured+biomimetic+%CE%B1-Fe2O3+on+degradation+of+tetracycline&search-within=Journal&facet-journal-id=40097](https://link.springer.com.ezproxy.javeriana.edu.co/search?query=Enhanced+UV-assisted+Fenton+performance+of+nanostructured+biomimetic+%CE%B1-Fe2O3+on+degradation+of+tetracycline&search-within=Journal&facet-journal-id=40097) (accessed on 15 August 2021). [CrossRef]
8. Murcia, J.J.; Ávila-Martínez, E.G.; Rojas, H.; Navío, J.A.; Hidalgo, M.C. Study of the E. coli elimination from urban wastewater over photocatalysts based on metallized TiO₂. *Appl. Catal. B* **2017**, *200*, 469–476. [CrossRef]
9. Murcia, J.J.; Arias, L.G.; Rojas, H.; Ávila-Martínez, E.G.; Jaramillo, C.; Lara, M.A.; Navío, J.A.; Hidalgo, M.C. Urban wastewater treatment by using Ag/ZnO and Pt/TiO₂ photocatalysts. *Environ. Sci. Pollut. Res.* **2019**, *26*, 4171–4179. [CrossRef] [PubMed]
10. Murcia, J.J.; Cely, A.C.; Rojas, H.; Hidalgo, M.C.; Navío, J.A. Fluorinated and Platinized Titania as Effective Materials in the Photocatalytic Treatment of Dyestuffs and Stained Wastewater Coming from Handicrafts Factories. *Catalysts* **2019**, *9*, 179. [CrossRef]
11. Murcia, J.J.; Hernández, J.S.; Rojas, H.; Moreno-Cascante, J.; Sánchez-Cid, P.; Hidalgo, M.C.; Navío, J.A.; Jaramillo-Páez, C. Evaluation of Au-ZnO, ZnO/Ag₂CO₃ and Ag-TiO₂ as Photocatalyst for Wastewater Treatment. *Top. Catal.* **2020**, *63*, 1286–1301. [CrossRef]
12. Murcia, J.J.; Hernández-Laverde, M.; Rojas, H.; Muñoz, E.; Navío, J.A.; Hidalgo, M.C. Study of the effectiveness of the flocculation-photocatalysis in the treatment of wastewater coming from dairy industries. *J. Photochem. Photobiol. A* **2018**, *358*, 256–264. [CrossRef]
13. Ming, G.; Zhenlu, L. Recent progress in Ag₃PO₄-based all-solid-state Z-scheme photocatalytic systems. *Chin. J. Catal.* **2017**, *38*, 1794–1803.
14. Martín-Gómez, A.N.; Navío, J.A.; Jaramillo-Páez, C.; Sánchez-Cid, P.; Hidalgo, M.C. Hybrid ZnO/Ag₃PO₄ photocatalysts, with low and high phosphate molar percentages. *J. Photochem. Photobiol. A* **2020**, *388*, 112196. [CrossRef]
15. Xu, H.; Dai, D.; Li, S.; Ge, L.; Gao, Y. In situ synthesis of novel Cu₂CO₃(OH)₂ decorated 2D TiO₂ nanosheets with efficient photocatalytic H₂ evolution activity. *Dalton Trans.* **2018**, *47*, 348–356. [CrossRef] [PubMed]
16. American Public Health Association (APHA). *Standard Methods for Examination of Water and Wastewater*, 22nd ed.; American Public Health Association/American Water Works Association/Water Environment Federation: Washington, DC, USA, 2012.
17. Rouquerol, F.; Rouquerol, J.; Sing, K.S.W.; Llewellyn, P.L.; Maurin, G. *Adsorption by Powders and Porous Solids: Principles, Methodology and Applications*, 2nd ed.; Elsevier/AP: Amsterdam, The Netherlands, 2014.
18. Jianguo, Y.; Jingrum, R. Facile preparation and enhanced photocatalytic H₂-production activity of Cu(OH)₂ cluster modified TiO₂. *Energy Environ. Sci.* **2011**, *4*, 1364–1371.
19. Ansari, M.A.; Khan, H.M.; Alzohairy, M.A.; Jalal, M.; Ali, S.G.; Pal, R.; Musarrat, J. Green synthesis of Al₂O₃ nanoparticles and their bactericidal potential against clinical isolates of multi-drug resistant *Pseudomonas aeruginosa*. *World J. Microbiol. Biotechnol.* **2015**, *31*, 153–164. [CrossRef] [PubMed]
20. Huang, S.; Xu, Y.; Xie, M.; Liu, Q.; Xu, H.; Zhao, Y.; He, M.; Li, H. A Z-scheme magnetic recyclable Ag/AgBr/CoFe₂O₄ photocatalyst with enhanced photocatalytic performance for pollutant and bacterial elimination. *RSC Adv.* **2017**, *7*, 30845–30854. [CrossRef]
21. Ray, S.K.; Dhakal, D.; Pandey, R.P.; Lee, S.W. Ag-BaMoO₄: Er³⁺/Yb³⁺ photocatalyst for antibacterial application. *Mater. Sci. Eng. C* **2017**, *78*, 1164–1171. [CrossRef]
22. Shirzad-Siboni, M.; Farrokhi, M.; Soltani, R.D.C.; Khataee, A.; Tajassosi, S. Photocatalytic Reduction of Hexavalent Chromium over ZnO Nanorods Immobilized on Kaolin. *Ind. Eng. Chem. Res.* **2014**, *53*, 1079–1087. [CrossRef]
23. Yang, H.; Lin, W.Y.; Rajeshwar, K. Homogeneous and heterogeneous photocatalytic reactions involving As(III) and As(V) species in aqueous media. *J. Photochem. Photobiol. A* **1999**, *123*, 137–143. [CrossRef]
24. Mohamed, R.M.; Barakat, M.A. Enhancement of Photocatalytic Activity of ZnO/SiO₂ by Nanosized Pt for Photocatalytic Degradation of Phenol in Wastewater. *Int. J. Photoenergy* **2012**, *2012*, 8. [CrossRef]

-
25. Wahyuni, E.; Aprilita, N.; Hatimah, H.; Wulandari, A.M.; Mudasir, M. Removal of Toxic Metal Ions in Water by Photocatalytic Method. *Am. Chem. Sci. J.* **2015**, *5*, 194. [[CrossRef](#)]
 26. Murcia, J.J.; Hidalgo, M.C.; Navío, J.A.; Araña, J.; Doña-Rodríguez, J.M. Study of the phenol photocatalytic degradation over TiO₂ modified by sulfation, fluorination, and platinum nanoparticles photodeposition. *Appl. Catal. B* **2015**, *179*, 305–312. [[CrossRef](#)]